



Chinese Pharmaceutical Association
Institute of Materia Medica, Chinese Academy of Medical Sciences

Acta Pharmaceutica Sinica B

www.elsevier.com/locate/apsb
www.sciencedirect.com



ORIGINAL ARTICLE

MANF brakes TLR4 signaling by competitively binding S100A8 with S100A9 to regulate macrophage phenotypes in hepatic fibrosis



Chao Hou^{a,b,†}, Dong Wang^{a,b,†}, Mingxia Zhao^{a,b,†}, Petek Ballar^c,
Xinru Zhang^{a,b}, Qiong Mei^{a,b}, Wei Wang^{a,b}, Xiang Li^{a,b},
Qiang Sheng^{a,b}, Jun Liu^{a,b}, Chuansheng Wei^{a,b}, Yujun Shen^{a,b},
Yi Yang^{a,b}, Peng Wang^{a,b}, Juntang Shao^{a,b}, Sa Xu^{a,b}, Fuyan Wang^{a,b},
Yang Sun^{d,*}, Yuxian Shen^{a,b,*}

^aSchool of Basic Medical Sciences, Anhui Medical University, Hefei 230032, China

^bBiopharmaceutical Research Institute, Anhui Medical University, Hefei 230032, China

^cDepartment of Biochemistry, Faculty of Pharmacy, Ege University, Izmir 35100, Turkey

^dState Key Laboratory of Pharmaceutical Biotechnology, School of Life Sciences, Nanjing University, Nanjing 210023, China

Received 11 February 2023; received in revised form 18 May 2023; accepted 13 June 2023

KEY WORDS

Hepatic fibrosis;
Mesencephalic astrocyte-
derived neurotrophic
factor;
Macrophage
differentiation;
Ly6C^{high} macrophages;
S100A8/S100A9;
TLR4;
NF- κ B pathway;
HSCs activation

Abstract The mesencephalic astrocyte-derived neurotrophic factor (MANF) has been recently identified as a neurotrophic factor, but its role in hepatic fibrosis is unknown. Here, we found that MANF was upregulated in the fibrotic liver tissues of the patients with chronic liver diseases and of mice treated with CCl₄. MANF deficiency in either hepatocytes or hepatic mono-macrophages, particularly in hepatic mono-macrophages, clearly exacerbated hepatic fibrosis. Myeloid-specific MANF knockout increased the population of hepatic Ly6C^{high} macrophages and promoted HSCs activation. Furthermore, MANF-sufficient macrophages (from WT mice) transfusion ameliorated CCl₄-induced hepatic fibrosis in myeloid cells-specific MANF knockout (MKO) mice. Mechanistically, MANF interacted with S100A8 to competitively block S100A8/A9 heterodimer formation and inhibited S100A8/A9-mediated TLR4–NF- κ B signal activation. Pharmacologically, systemic administration of recombinant human MANF significantly alleviated CCl₄-induced hepatic fibrosis in both WT and hepatocytes-specific MANF knockout (HKO) mice. This study reveals a mechanism by which MANF targets S100A8/A9–TLR4 as a “brake” on the

*Corresponding authors.

E-mail addresses: shenyx@ahmu.edu.cn (Yuxian Shen), yangsun@nju.edu.cn (Yang Sun).

†These authors made equal contributions to this work.

Peer review under the responsibility of Chinese Pharmaceutical Association and Institute of Materia Medica, Chinese Academy of Medical Sciences.

<https://doi.org/10.1016/j.apsb.2023.07.027>

2211-3835 © 2023 Chinese Pharmaceutical Association and Institute of Materia Medica, Chinese Academy of Medical Sciences. Production and hosting by Elsevier B.V. This is an open access article under the CC BY-NC-ND license (<http://creativecommons.org/licenses/by-nc-nd/4.0/>).

upstream of NF- κ B pathway, which exerts an impact on macrophage differentiation and shed light on hepatic fibrosis treatment.

© 2023 Chinese Pharmaceutical Association and Institute of Materia Medica, Chinese Academy of Medical Sciences. Production and hosting by Elsevier B.V. This is an open access article under the CC BY-NC-ND license (<http://creativecommons.org/licenses/by-nc-nd/4.0/>).

1. Introduction

Chronic liver diseases represent a class of chronic hepatic disorders that usually begin with liver injury and inflammation. Hepatic chronic inflammatory events activate hepatic stellate cells (HSCs), myofibroblasts differentiation, and ECM protein accumulation, eventually resulting in hepatic fibrosis^{1–3}. HSCs produce and secrete a large amount of collagen-I and -III⁴. In addition to increasing ECM protein synthesis, HSCs express tissue inhibitors of metalloproteinase (TIMPs), which restrain the secretion and activity of metalloproteinases (MMPs) that promote ECM protein degradation^{5,6}. Multiple pathological factors such as viral infection, excessive drinking, and drug abuse can lead to hepatic inflammation, which could further progress to hepatic fibrosis, cirrhosis, and even hepatic carcinoma^{7–9}. Identification and characterization of the pivotal anti-inflammatory factors in liver is an urgent demand for the prevention and treatment of chronic liver diseases.

Mesencephalic astrocyte-derived neurotrophic factor (MANF), initially identified as a neurotrophic factor^{10–13}, is an endoplasmic reticulum (ER) stress inducible protein that is extensively expressed in liver^{14–16}. Previous research has reported that hepatic MANF expression decreases with aging¹⁷. MANF supplementation can relieve liver aging, prevent hepatic steatosis and restore metabolic dysfunction¹⁷. Our previous studies demonstrated that MANF is upregulated in inflammatory diseases and attenuates inflammation by inhibiting NF- κ B signaling pathway^{18,19}. Furthermore, MANF has been found to play a protective role against alcohol¹⁵, rifampicin¹⁶, and ischemia/reperfusion-induced liver injury¹⁴. Recently, we also reported that MANF, whose level is significantly reduced in the tissues of hepatocellular carcinoma (HCC), inhibited the progression of HCC by suppressing NF- κ B/Snail signaling pathway²⁰. However, the level of MANF in the hepatic fibrosis, which is the stage prior to HCC, and the role of MANF in this stage need to be investigated. In this study, we evaluated the level of MANF in patients with Chronic liver diseases and in mice with carbon tetrachloride (CCl₄)-induced hepatic fibrosis, and the effect of MANF on liver fibrosis was elucidated by using MANF knockout mice, macrophages transfusion and recombinant human MANF (rhMANF). Meanwhile, the efficacy of hepatocyte- and macrophage-derived MANF was compared, and the underlying mechanism by which hepatic macrophage-derived MANF manipulated hepatic macrophages to differentiate into anti-inflammatory phenotypes was investigated.

2. Materials and methods

2.1. Patients

Hepatic tissues were collected from 8 patients with hepatitis, 7 patients with hepatic fibrosis, and 7 patients with hepatic cirrhosis by liver puncture biopsy from the First Affiliated Hospital of

Anhui Medical University (Hefei, China). Immunohistochemistry assay was used to examine the level of MANF in human hepatic tissues. All the experiments related to human tissues were conducted in accordance with the Helsinki criteria and were also approved by the Ethics Committees of Anhui Medical University with the approval number 20200282. The informed consent was obtained from all involved patients.

2.2. Mice

Manf^{flox/flox} mice bearing loxP sites flanking exons 3 of the *Manf* gene on the C57BL/6 background were provided by Prof. Jia Luo of Kentucky University. *Manf*^{flox/flox} mice were cross-bred with Alb-Cre or Lyz2-Cre to specifically knock out *Manf* gene in hepatocytes (HKO) or myeloid cells (MKO). The mating and reproduction of HKO and MKO mice was completed by Gem-Pharmatech Co., Ltd. (Nanjing, China). The littermate *Manf*^{flox/flox} mice were used as wild type (WT) control. SPF-class animal laboratory was used to raise and breed mice. All mice experiments were performed according to protocols approved by the Animal Ethics Committee of Anhui Medical University with the approval number LLSC20200022.

2.3. CCl₄-induced hepatic fibrosis model

The male WT, MKO, and HKO mice at 6-week-old age were used for establishing hepatic fibrosis model. Carbon tetrachloride (CCl₄) dissolved in olive oil was administrated by intraperitoneal injection three times a week for 8 weeks at a dose of 0.5 μ L/g. All mice were sacrificed 24 h after the final CCl₄ injection to acquire livers and serum samples. The body weight of all mice was recorded weekly.

2.4. Primary cell isolation and culture

Peritoneal macrophages were isolated from WT and MKO mice. After anesthetization and disinfection, 5 mL 1 \times PBS was injected to mice's abdomen for 5 min. Cell suspensions were collected by centrifugation at 500 \times g for 5 min. Then, peritoneal cells were cultured in DMEM with 20% fetal calf serum for 2 h. Non-adherent cells were removed, and the remaining adherent cells were collected.

Hepatic macrophages and hepatic stellate cells (HSCs) were prepared and cultured as previously described²¹. Briefly, mice were perfused with Hank's buffer with EGTA (0.5 mmol/L) for 3 min (60 rpm), then perfused with 15 mL Hank's buffer containing collagenase IV (0.2 g/L) via hepatic portal vein for 3 min (60 rpm). Liver tissues were collected and incubated on rotary shaker (200 rpm) for 20 min. For hepatic macrophages collection and treatment, the dispersed liver cell suspensions were performed by gradient centrifugation with 25% and 50% Percoll (P1644-1L, Sigma–Aldrich). Primary hepatic macrophages were cultured in

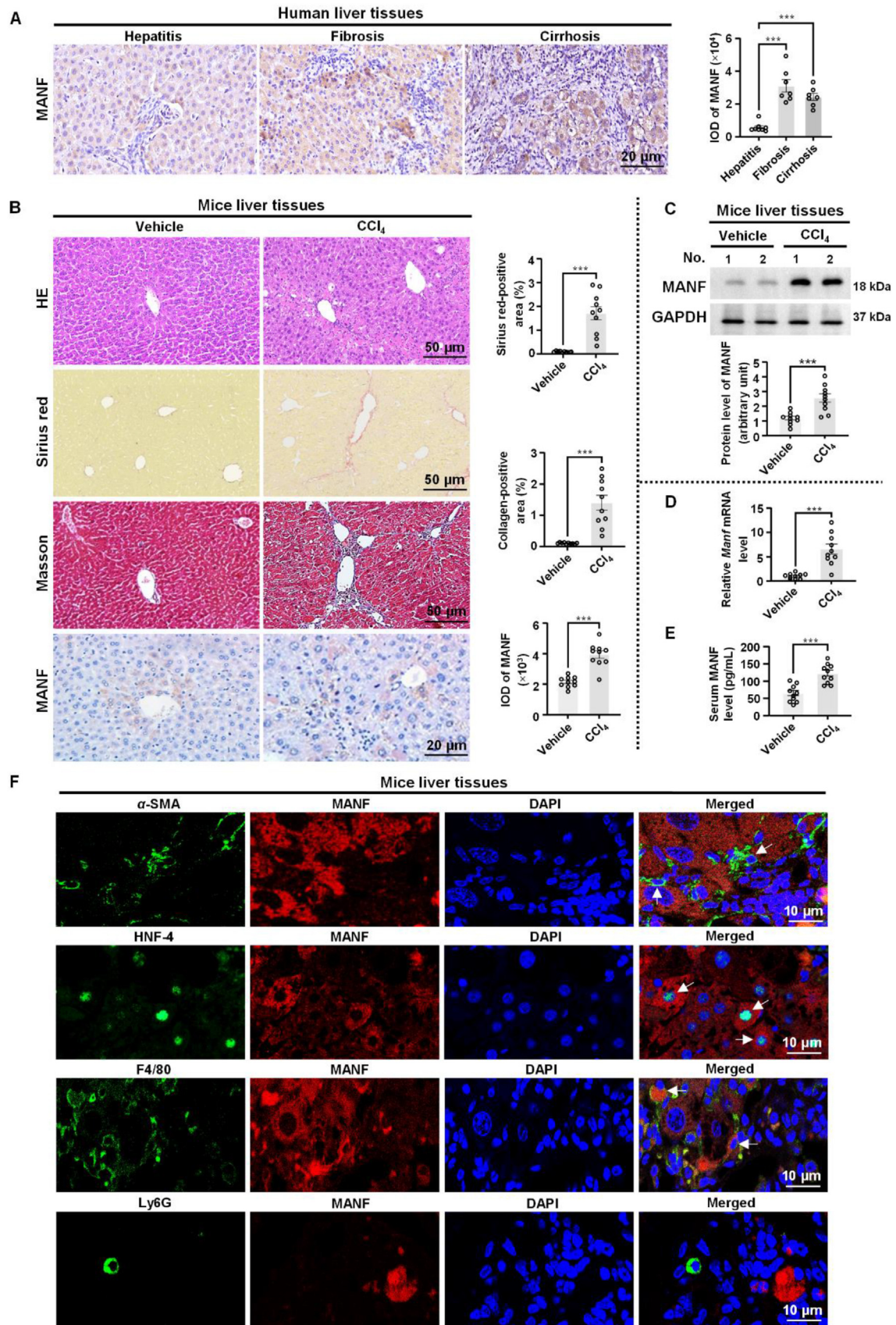


Figure 1 MANF expression is upregulated in fibrotic liver tissues. (A) MANF level in hepatic tissues of the patients with hepatitis ($n = 8$), hepatic fibrosis ($n = 7$), and hepatic cirrhosis ($n = 7$) detected by using immunohistochemistry assay, and the integral optical density were calculated. (B) HE, Sirius red, and Masson staining in CCl₄-treated fibrotic liver tissues were performed, and the positive area was calculated.

DMEM with 20% fetal calf serum. Hepatic macrophages isolated from WT and MKO mice were stimulated by LPS (500 ng/mL) for 6 h, then the medium supernatant of macrophages was collected to treat primary HSCs isolated from WT mice. For HSCs collection and treatment, the dispersed liver cells suspension was performed by gradient centrifugation with 11.5% and 20% optiPrep (Axis-Shield, Norway). Primary HSCs were cultured in the special DMEM for HSCs culture (CM-0116, Procell, China), then stimulated by TNF- α (20 ng/mL) for 6 h after pretreatment of recombinant human MANF (rhMANF) (0, 5, 10, 20 μ g/mL) for 2 h.

2.5. Macrophages transfection

Macrophages transfection were performed following a previously described protocol²². The peritoneal macrophages were isolated from WT and MKO mice and then were injected into MKO mice by tail vein with 1×10^6 cells after 4-week CCl₄ injection. Twenty-four hours after the last CCl₄ injection, the mice were sacrificed and the liver tissues and serum samples were collected.

2.6. Recombinant human MANF treatment

The expression and purification of rhMANF were performed as previously described¹³. After 8 weeks CCl₄ injection, rhMANF (0, 15, 30, 60 μ g/mouse) were administrated through tail vein twice a week for 2 weeks. Twenty-four hours after the last rhMANF injection, mice were sacrificed to collect liver tissues and serum samples.

2.7. Serum AST and ALT assay

Serum AST and ALT levels were detected by using AST (Jiancheng Bioengineering Institute, Nanjing, China, C010-2-1) and ALT assay kits (Jiancheng Bioengineering Institute, Nanjing, China, C009-2-1) according to the manufacturer's instructions.

2.8. Sirius red staining

Paraffin sections of hepatic tissues from WT, MKO, and HKO mice were used to perform Sirius red staining. Briefly, after deparaffinization, rehydration was performed in 100%, 90%, 80%, and 70% ethanol, followed by Sirius red staining (Solarbio, G1472) for 1 h and rinsing for 30 min. Sirius red staining images were obtained by Olympus Microscope BX53/IX71.

2.9. Masson staining

Masson staining was performed for paraffin sections of hepatic tissues from WT, MKO, and HKO mice using Masson staining kit (Solarbio, G1346). Briefly, paraffin sections were used for deparaffination and rehydration in 100%, 90%, 80%, and 70% ethanol, followed by Weigert's iron hematoxylin staining, differentiation acidic ethanol solution treatment, Masson solution treatment, and ponceau acid Fuchs solution treatment in sequence. After rinsing by weak acid buffer and phosphomolybdic acid

solution, aniline blue staining and ethanol dehydration were performed. Masson staining images were obtained by Olympus Microscope BX53/IX71.

2.10. Immunohistochemistry

Immunohistochemistry was performed for hepatic tissues according to the previous research²⁰. Firstly, hepatic tissues were fixed in 10% formaldehyde for 24 h. After paraffin embedding, paraffin sections were produced, followed by deparaffinization in dimethylbenzene for 2 h. Then, rehydration was performed in 100%, 90%, 80%, and 70% ethanol. For hematoxylin-eosin (HE) staining, hematoxylin and eosin were used. For immunohistochemical staining, paraffin sections were stained by the indicated antibodies of MANF, HMGB1, TGF- β 1, α -SMA, MMP2, MMP9, S100A8, S100A9, TLR4, TIMP1, TIMP2, CCL2, CX3CL1, and phosphorylated NF- κ B p65, followed by 3,3'-diaminobenzidinetetrahydrochloride (DAB) and hematoxylin staining. Immunohistochemical images were obtained by Olympus Microscope BX53. The involved antibodies were included in Supporting Information Table S1.

2.11. Enzyme-linked immunosorbent assay (ELISA)

ELISA was used to examine the levels of TGF- β 1, TNF- α , Hyaluronan, IL-1 β , S100A8, and S100A9 in serum from WT, MKO, and HKO mice according to manufacturer's instruction. The utilized ELISA Kits included Mouse TGF- β 1 ELISA Kit (R&D Systems, Minneapolis, USA, MB100B), Mouse TNF- α ELISA Kit (Abcam, ab208348), Mouse IL-1 β ELISA Kit (Abcam, ab197742), Mouse CCL2 ELISA Kit (Abcam, ab208979), Mouse S100A8 ELISA Kit (Abcam, ab263886), Mouse S100A9 ELISA Kit (Abcam, ab213887), Mouse Hyaluronan ELISA Kit (Jiyinmei Biological Technology, Wuhan, China, JYM0514Mo), and Mouse MANF ELISA Kit (Cloud-Clone Corp, Wuhan, China, SEC300Mu).

2.12. Immunofluorescent staining

Immunofluorescent staining was performed according to the previous research^{14,16,20}. For paraffin sections, deparaffination and rehydration were performed. Then, paraffin sections and cell culture slides were incubated by 5% BSA for 30 min, followed by antibodies staining for 2 h. DAPI was used for nuclei staining. Immunofluorescent staining images were obtained by Zeiss LSM800. The involved antibodies were included in Table S1.

2.13. Western blot

Cell lysates and protein samples were used for the reduced sodium dodecyl sulfate polyacrylamide gel electrophoresis (SDS-PAGE). The loading quantity for each sample was 10 μ g total protein. After protein separation, protein bands were transferred to PVDF membrane. Then, 5% BSA and antibodies were used for membrane incubation. The target protein bands were visualized by

MANF was detected by immunohistochemistry and the integral optical density was calculated ($n = 10$). (C, D) MANF protein (C) and mRNA (D) levels in CCl₄-treated fibrotic liver tissues were detected by Western blot and qPCR ($n = 10$), respectively. The relative MANF levels were calculated. (E) Serum MANF was detected by ELISA. (F) Double labeled immunofluorescence was performed to detect the colocalization of MANF (red) with α -SMA (green), HNF-4 (green), F4/80 (green), and Ly6G (green) in fibrotic liver tissues ($n = 10$). DAPI (blue) was used to stain nuclei. Data are expressed as mean \pm SEM. *** $P < 0.001$. WT, wild type; CCl₄, carbon tetrachloride.

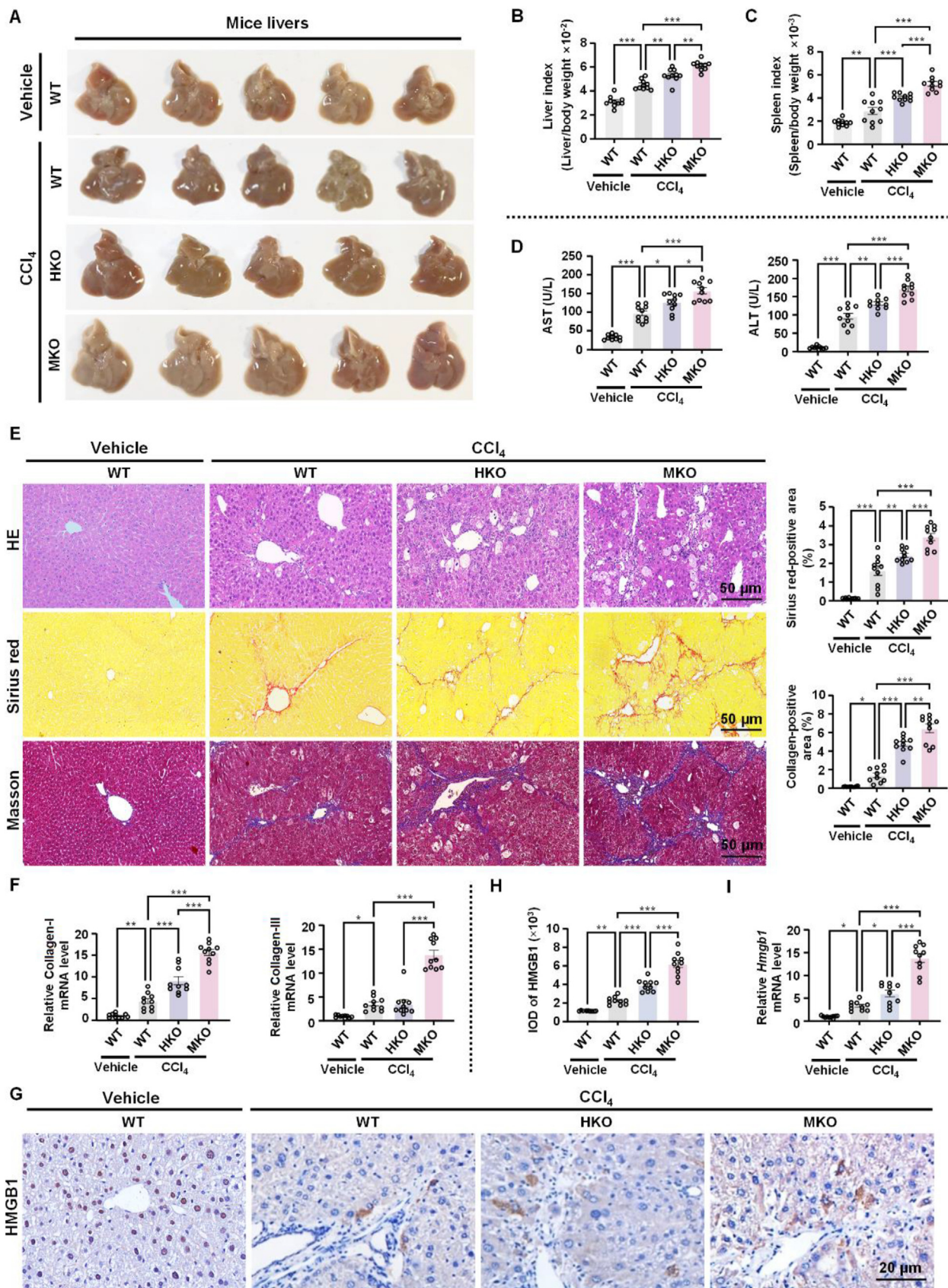


Figure 2 MANF knockout in hepatocytes or myeloid cells exacerbates CCl₄-induced hepatic fibrosis. (A) The morphology of livers. (B) Liver index. (C) Spleen index. (D) Serum AST and ALT levels. (E) HE, Sirius red, and Masson staining. The positive area was calculated. (F) Collagen-I

Chemscope 6000 pro touch imaging system. The involved antibodies were included in Table S1.

2.14. Quantitative real time polymerase chain reaction (qPCR)

Trizol reagent was used for total RNA extraction, then reverse transcription was performed by PrimeScript RT reagent Kit (TaKaRa Bio, Dalian, China) according to manufacturer's instruction. The involved primers were included in Supporting Information Table S2.

2.15. Flow cytometry

Hepatic tissues from WT, MKO, and HKO mice were used to produce cell suspensions for flow cytometry assay. Cells were blocked by 1% rat serum in $1 \times$ PBS, followed by staining with antibodies for 30 min. After washing by $1 \times$ PBS, cell suspensions were analyzed by BD FACS Celesta. The involved antibodies were included in Table S1.

2.16. Co-immunoprecipitation (Co-IP)

RAW264.7 cells were stimulated with LPS (0.5 μ g/mL) for 6 h. Cell lysates were prepared in IP lysis buffer containing 50 mmol/L HEPES (pH 7.4), 150 mmol/L NaCl, 0.1% Triton X-100, 2 mmol/L EGTA, and cocktail (protease inhibitor). Co-immunoprecipitation was performed according to the previous research²⁰. After pre-cleaning with protein A/G plus-agarose, lysates were incubated with anti-MANF or anti-S100A8 antibodies overnight at 4 °C. Protein A/G plus-agarose was added, followed by washing in Co-IP washing buffer (20 mmol/L Tris-HCl, pH 7.6, 100 mmol/L NaCl, and 1 mmol/L EDTA). Co-IP results were analyzed by SDS-PAGE and immunoblotting. The involved antibodies were included in Table S1.

2.17. Immunoprecipitation-coupled mass spectrometry analysis

Immunoprecipitation was performed according our previous study²³. Briefly, immunoprecipitation was performed on HepG2 cell lysates using anti-MANF antibody (ab67271, Abcam) or isotype control antibody (CST3900, Cell Signaling Technology). Protein samples were used for the SDS-PAGE, and the gel was processed by Shanghai Applied Protein Technology Company for immunoprecipitation-mass spectrometry (IP-MS). LC-MS (Q Exactive™ Quadrupole-Orbitrap™ Mass Spectrometer and Easy-nLC 1000 chromatograph, Thermo Fisher) was performed on the peptide mixture obtained from trypsin digestion of protein samples. The peptide sequence was identified by bioinformatics analysis using MASCOT software. The mass spectrometry proteomics data have been deposited in the ProteomeXchange Consortium (<http://proteomecentral.proteomexchange.org>) with the dataset identifier PXD035967.

2.18. Statistics

Data are expressed as the mean \pm standard error of mean (SEM). For comparisons between two groups, two-tailed Student's *t*-test

was used to determine statistical significance. For multiple comparisons, two-way ANOVA followed by Tukey's *post hoc* test was used to determine statistical significance. $P < 0.05$ (One asterisk, *) indicates the significant difference. Two asterisks (**) mean $P < 0.01$, three asterisks (***) mean $P < 0.001$. The integral optical density, Sirius red positive area, and collagen fibers area were calculated by Image J. Data are representative of three independent experiments.

3. Results

3.1. MANF expression is upregulated in hepatic fibrosis

Our previous research has reported that the MANF level was increased in the serum of hepatitis B virus-infected hepatitis and hepatic fibrosis patients compared to healthy individuals²⁴. Consistently, MANF expression was observed in the paraffin-embedded liver tissues from 8 hepatitis, 7 hepatic fibrosis, and 7 hepatic cirrhosis patients. The results revealed that hepatic MANF protein levels in the patients with fibrosis and cirrhosis were significantly increased than that in the patients with hepatitis (Fig. 1A). To verify the correlation between MANF level and hepatic fibrosis, firstly CCl₄-induced hepatic fibrosis mouse model was established. As shown in Fig. 1B, the significant liver injury and collagen deposition reflected by HE, Sirius red, and Masson staining were found to correlate well with MANF levels. Furthermore, MANF protein and mRNA levels were significantly increased in the fibrotic liver tissues (Fig. 1C and D), indicating hepatic fibrosis promoted MANF expression. The serum MANF level was significantly increased in mice with hepatic fibrosis (Fig. 1E). The double-labeled immunofluorescent staining exhibited that MANF was co-localized with HNF-4 and F4/80, but not with α -SMA and Ly6G in liver tissues (Fig. 1F), suggesting that MANF was specifically expressed in hepatocytes and hepatic macrophages, but not in HSCs and hepatic granulocytes. These results, together with our previous findings, indicate that hepatic fibrosis can upregulate the expression and secretion of MANF, which is mainly derived from hepatocytes and hepatic macrophages.

3.2. MANF knockout in hepatocytes or myeloid cells exacerbates CCl₄-induced hepatic fibrosis

As MANF mainly expresses in hepatocytes and macrophages which are the two major cell types expressing MANF in the liver, we constructed HKO and MKO mice, respectively, to elucidate the significance of MANF upregulation in liver fibrosis. The efficiency of MANF knockout was identified by immunoblotting and immunohistochemistry, which showed that MANF was specifically knocked out in the hepatocytes in HKO mice (Supporting Information Fig. S1A, S1C and S1D) and in the myeloid cells, including peritoneal macrophages in MKO mice (Fig. S1B, S1C and S1D). Even in the fibrotic liver tissues, MANF level was significantly reduced in both HKO and MKO mice compared to WT mice (Fig. S1E and S1F). We also found MANF knockout, either in hepatocytes or myeloid cells, did not affect the liver and spleen indexes, serum ALT level, and liver histology (Supporting

and -III mRNA levels in hepatic tissues detected by qPCR. (G) HMGB1 protein level detected by immunohistochemistry. (H) The quantitative data in panel G. (I) *Hmgbl* mRNA level detected by qPCR. Data are expressed as mean \pm SEM, $n = 10$; * $P < 0.05$, ** $P < 0.01$, *** $P < 0.001$. WT, wild type; HKO, MANF knockout in hepatocytes; MKO, MANF knockout in myeloid cells; CCl₄, carbon tetrachloride.

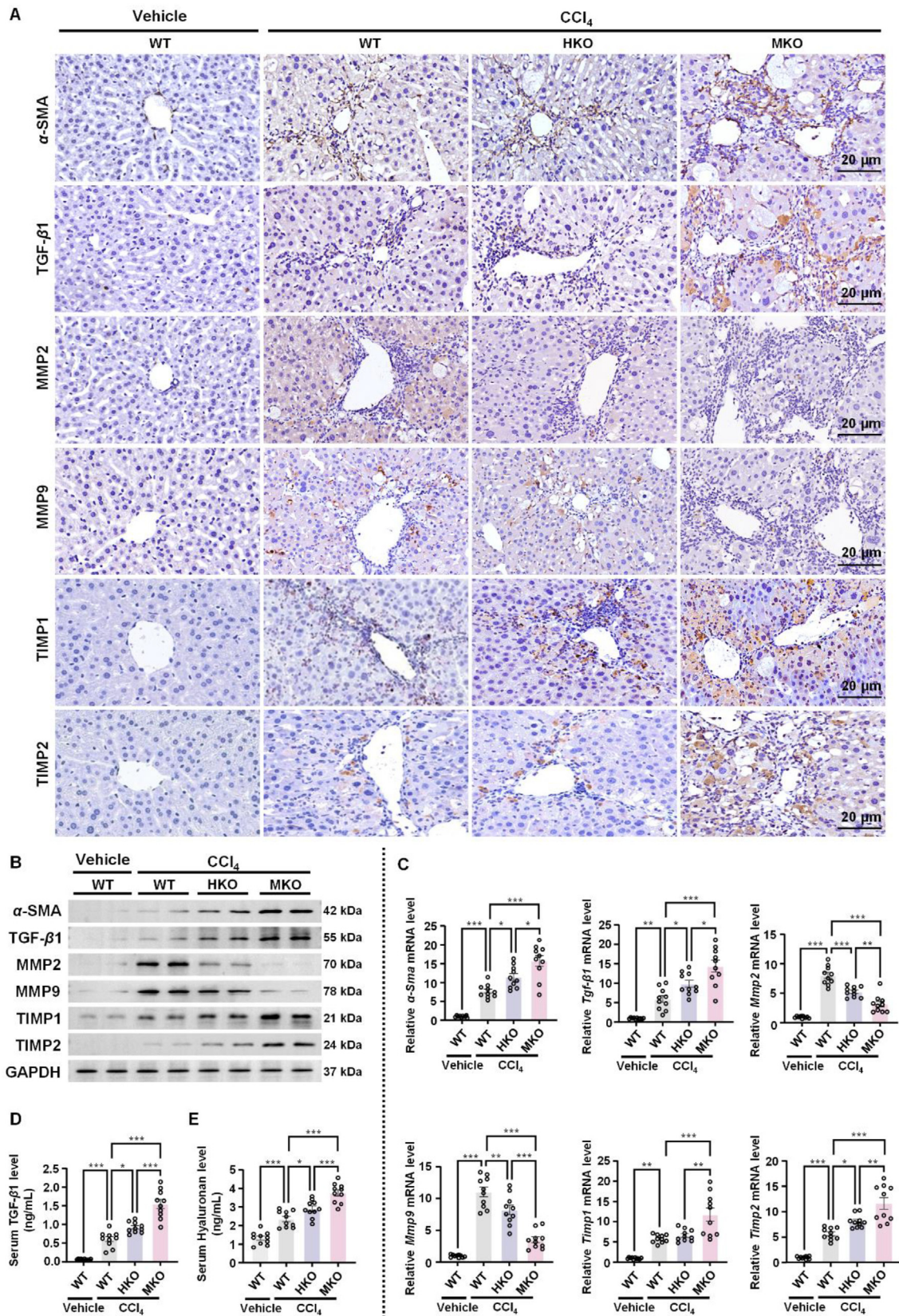


Figure 3 Myeloid cell-specific MANF knockout promotes CCl₄-induced HSCs activation. (A–C) The levels of α -SMA, TGF- β 1, MMP2, MMP9, TIMP1, and TIMP2 in fibrotic liver tissues were detected by using immunohistochemistry (A), Western blot (B), and qPCR (C). (D, E) Serum TGF- β 1 (D) and hyaluronan (E) levels were detected by ELISA. Data are expressed as mean \pm SEM, $n = 10$; * $P < 0.05$, ** $P < 0.01$, *** $P < 0.001$. WT, wild type; HKO, MANF knockout in hepatocytes; MKO, MANF knockout in myeloid cells; CCl₄, carbon tetrachloride.

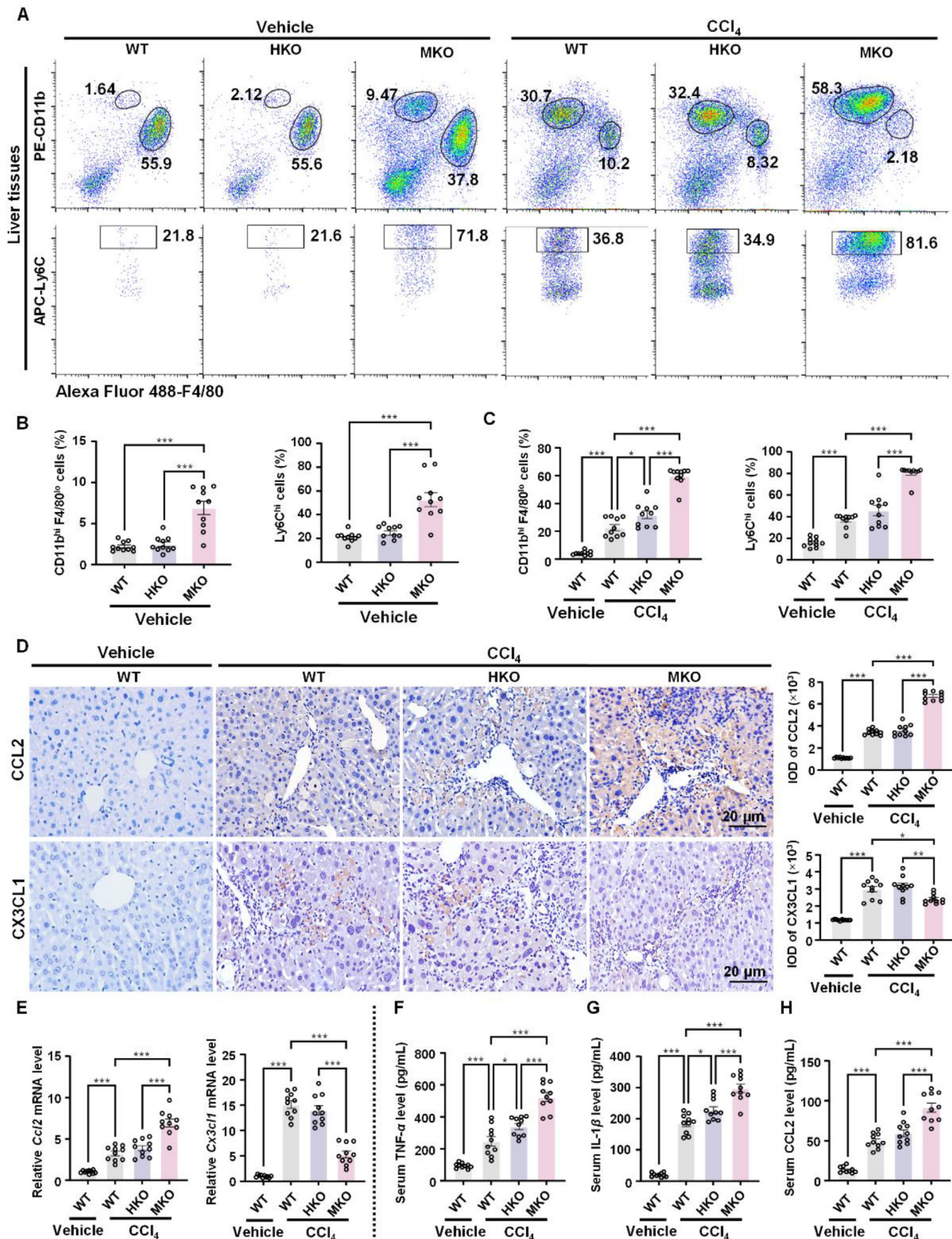


Figure 4 Myeloid MANF knockout promotes Ly6C^{high} macrophages recruitment in liver. (A) Myeloid MANF deficiency increased the proportion of hepatic CD11b^{high}F4/80^{low}Ly6C^{high} mono-macrophages detected by flow cytometry. (B, C) The quantitative data in vehicle-treated (B) and CCl₄-treated (C) mice were calculated. (D, E) The expressions of CCL2 and CX3CL1 were detected by immunohistochemistry (D) and qPCR (E). The integral optical density was calculated. (F–H) Myeloid MANF deficiency increased serum TNF- α (F), IL-1 β (G), and CCL2 (H) levels detected by ELISA. Data are expressed as mean \pm SEM, $n = 10$; * $P < 0.05$, ** $P < 0.01$, *** $P < 0.001$. WT, wild type; HKO, MANF knockout in hepatocytes; MKO, MANF knockout in myeloid cells; CCl₄, carbon tetrachloride.

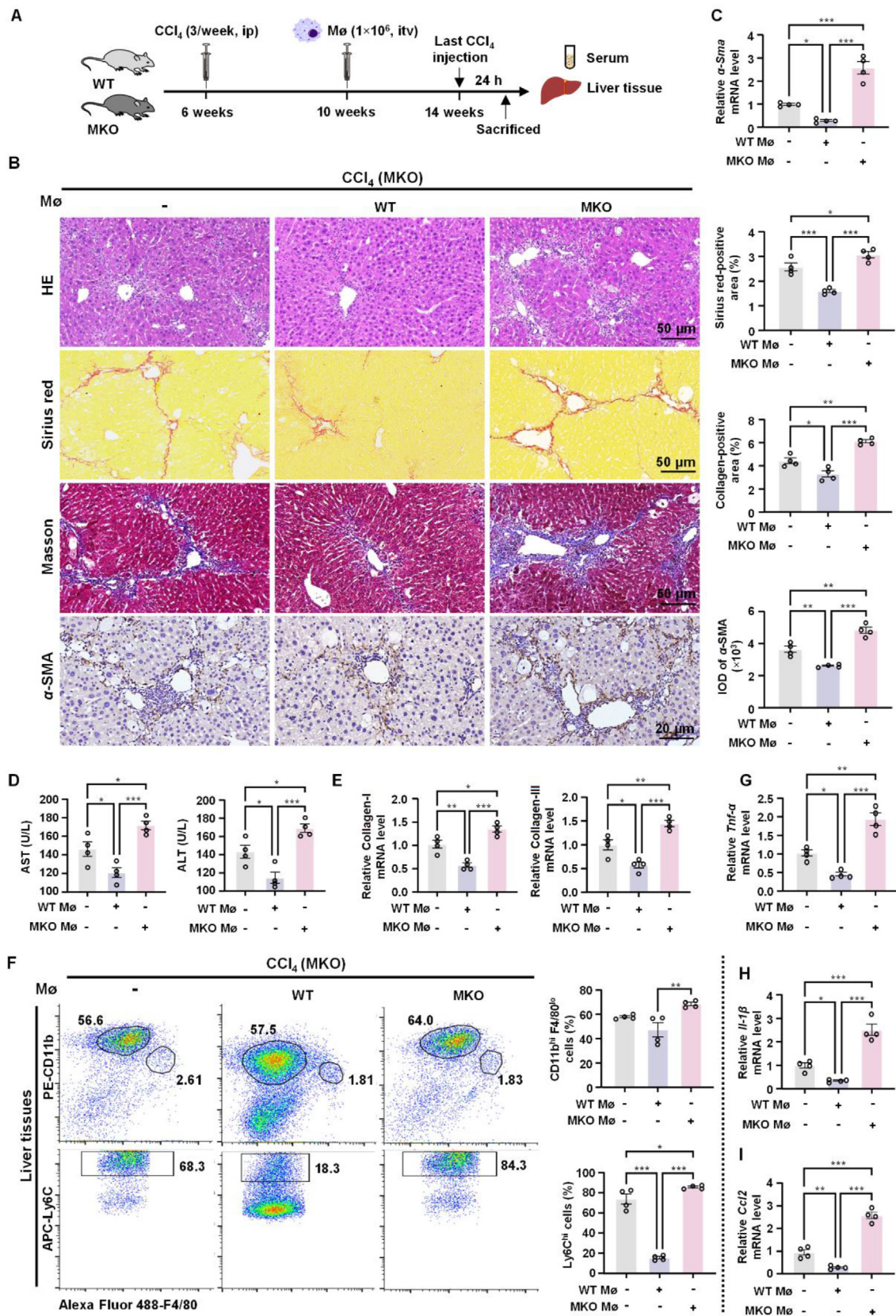


Figure 5 MANF-sufficient macrophages transfusion alleviates CCl₄-induced liver fibrosis in MKO mice. (A) Strategy for macrophages transfusion. (B) MANF-sufficient macrophages transfusion alleviated CCl₄-induced hepatic fibrosis in MKO mice. HE, Sirius red, and Masson staining were performed. α -SMA were detected by immunohistochemistry. The staining-positive area and integral optical density were calculated. (C) Hepatic α -Sma mRNA was detected by qPCR. (D–F) MANF-sufficient macrophages transfusion decreased serum AST and ALT levels (D),

Information Fig. S2A–S2E). Only serum AST level was increased in MKO mice but not in HKO mice compared to WT mice (Fig. S2D). However, after CCl₄ treatment, all these tested parameters, along with collagen-I and -III levels, were dramatically increased in MKO and HKO mice, especially in MKO mice compared to WT mice (Fig. 2A–F), suggesting that MANF deficiency in hepatocytes and myeloid cells exacerbated hepatic fibrosis. We also found that the protein and mRNA levels of HMGB1, a damage-associated molecular pattern involved in hepatic fibrosis by stimulating HSCs migration²⁵, were elevated in HKO and MKO mice than that in WT mice after treatment with CCl₄ (Fig. 2G–I and Fig. S2F). The percentage of nuclear HMGB1-positive cells was extremely decreased in MKO mice than that in WT and HKO mice (Fig. S2G). These results suggest that MANF derived from hepatocytes or hepatic macrophages may exert a protective effect in response to CCl₄ challenge, and MANF may play a more important role in hepatic macrophages.

3.3. Myeloid cell-specific MANF knockout promotes CCl₄-induced HSCs activation

Next, we investigated the effect of MANF on HSCs activation. Due to the absence of MANF in HSCs, we assumed that MANF might exert its effect on HSCs *via* paracrine secretion. Therefore, we used HKO and MKO mice to observe the effects of MANF deficiency on HSCs activation by detecting the levels of relevant factors, including α -SMA, which is an important biomarker for HSCs activation, which plays a crucial role in the development of liver fibrosis²⁶. TGF- β 1 is considered as a pro-hepatic fibrosis factor since it activates HSCs^{27,28}. We found that MANF knockout caused no significant changes in the levels of α -SMA, TGF- β 1, MMP2, MMP9, TIMP1, and TIMP2 neither in hepatocytes nor in myeloid cells of the liver tissues (Fig. S4A and S4B). However, under the challenge of CCl₄, the levels of α -SMA, TGF- β 1, TIMP1, and TIMP2 were increased, whereas the levels of MMP2 and MMP9 were decreased in the fibrotic liver tissues of HKO and MKO compared to that in WT mice, and the changes of these parameters in MKO mice were more significant than in HKO mice (Fig. 3A–C, Fig. S3A and S3B). Meanwhile, the serum TGF- β 1 level was increased in the fibrotic liver tissues of HKO and MKO mice compared with that in WT mice (Fig. 3D). We also found increased levels of serum Hyaluronan, a valuable biomarker of liver fibrosis²⁹, in HKO and MKO mice (Fig. 3E). These results indicate MANF deficiency in hepatocytes and hepatic mono-macrophages can promote HSCs activation at significantly different levels in liver fibrosis. The effect of MANF deficiency on HSCs activation in MKO mice is clearly stronger than that in HKO mice, suggesting that MANF derived from hepatic mono-macrophages may play a more important role in HSCs activation than hepatocytes-derived MANF.

3.4. Myeloid MANF knockout promotes Ly6C^{high} macrophages recruitment in liver

The above data revealed that macrophage-derived MANF plays a more important role than hepatocyte-derived MANF in HSCs

activation and liver fibrosis. Considering the crucial role of Ly6C^{high} macrophages in hepatic fibrosis³⁰, we investigated the proportional change of hepatic macrophage subpopulations during the hepatic fibrosis process. The results showed that the proportions of hepatic CD11b^{high}F4/80^{low} macrophages and Ly6C^{high}F4/80^{low} macrophages in MKO mice with liver fibrosis were 58.3% and 81.6%, respectively, which were markedly increased compared with WT mice (30.7%, 36.8%) and HKO mice (32.4%, 34.9%) (Fig. 4A, right panel; Fig. 4C). Interestingly, the proportions of hepatic CD11b^{high}F4/80^{low} and Ly6C^{high}F4/80^{low} macrophages in MKO mice untreated with CCl₄ were also higher than that in WT and HKO mice (Fig. 4A, left panel; Fig. 4B), indicating endogenous MANF of myeloid cells may restrict the differentiation of mono-macrophages into pro-inflammatory macrophage subtype.

A higher level of CCL2 and lower level of CX3CL1 were found in the fibrotic liver tissues of MKO mice than that of WT and HKO mice, while there was no difference between WT and HKO mice (Fig. 4D and E). Additionally, without CCl₄ challenge, CCL2 level was also increased in MKO mice compared to WT and HKO mice (Supporting Information Fig. S5A and S5B). Furthermore, higher serum levels of TNF- α , IL-1 β , and CCL2 were found in MKO mice with hepatic fibrosis compared to HKO mice (Fig. 4F–H). These findings suggest that myeloid MANF knockout enhances Ly6C^{high} pro-inflammatory macrophages differentiation and promotes their recruitment in the liver.

3.5. MANF-sufficient macrophages transfusion ameliorates CCl₄-induced liver fibrosis in MKO mice

To further confirm the effect of MANF on macrophages differentiation and liver fibrosis, we isolated the peritoneal macrophages from WT and MKO mice and then transfused them *via* the tail vein to WT and MKO mice with liver fibrosis following a 4-week CCl₄ injection (Fig. 5A). After an additional 4-week CCl₄ injection, the mice were sacrificed, the liver tissues and serum samples were collected for further detection. We found that transfusion of MANF-sufficient macrophages (from WT mice) ameliorated the CCl₄-induced hepatic injury and fibrosis in MKO mice (Fig. 5B–E), while transfusion of MANF-deficient macrophages (from MKO mice) aggravated hepatic injury and fibrosis in WT mice (Fig. S6A–S6C). Further flow cytometry analysis showed that transfusion of MANF-sufficient macrophages (from WT mice) dramatically reduced the population of liver Ly6C^{high}F4/80^{low} macrophages in MKO mice (Fig. 5F); conversely, transfusion of MANF-deficient macrophages (from MKO mice) elevated the population of liver Ly6C^{high}F4/80^{low} macrophages in WT mice (Fig. S6D). Consistently, the expressions of pro-inflammatory cytokines in hepatic tissues, including *Tnf- α* , *Il-1 β* , and *Ccl2*, were downregulated after MANF-sufficient macrophages transfusion to MKO mice (Fig. 5G–I), while upregulated after MANF-deficient macrophages transfusion to WT mice (Fig. S6E–S6G). These results further support the above notion that macrophage-derived MANF plays an important role in hepatic proinflammatory macrophage recruitment and fibrosis.

hepatic Collagen-I and -III mRNA levels detected by qPCR (E), and hepatic proportion of CD11b^{high}F4/80^{low}Ly6C^{high} mono-macrophages detected by flow cytometry (F) in MKO mice. (G–I) MANF-sufficient macrophages transfusion decreased hepatic mRNA expressions of *Tnf- α* (G), *Il-1 β* (H), and *Ccl2* (I) detected by qPCR in MKO mice. Data are expressed as mean \pm SEM, $n = 4$; * $P < 0.05$, ** $P < 0.01$, *** $P < 0.001$. WT, wild type; MKO, MANF knockout in myeloid cells; CCl₄, carbon tetrachloride.

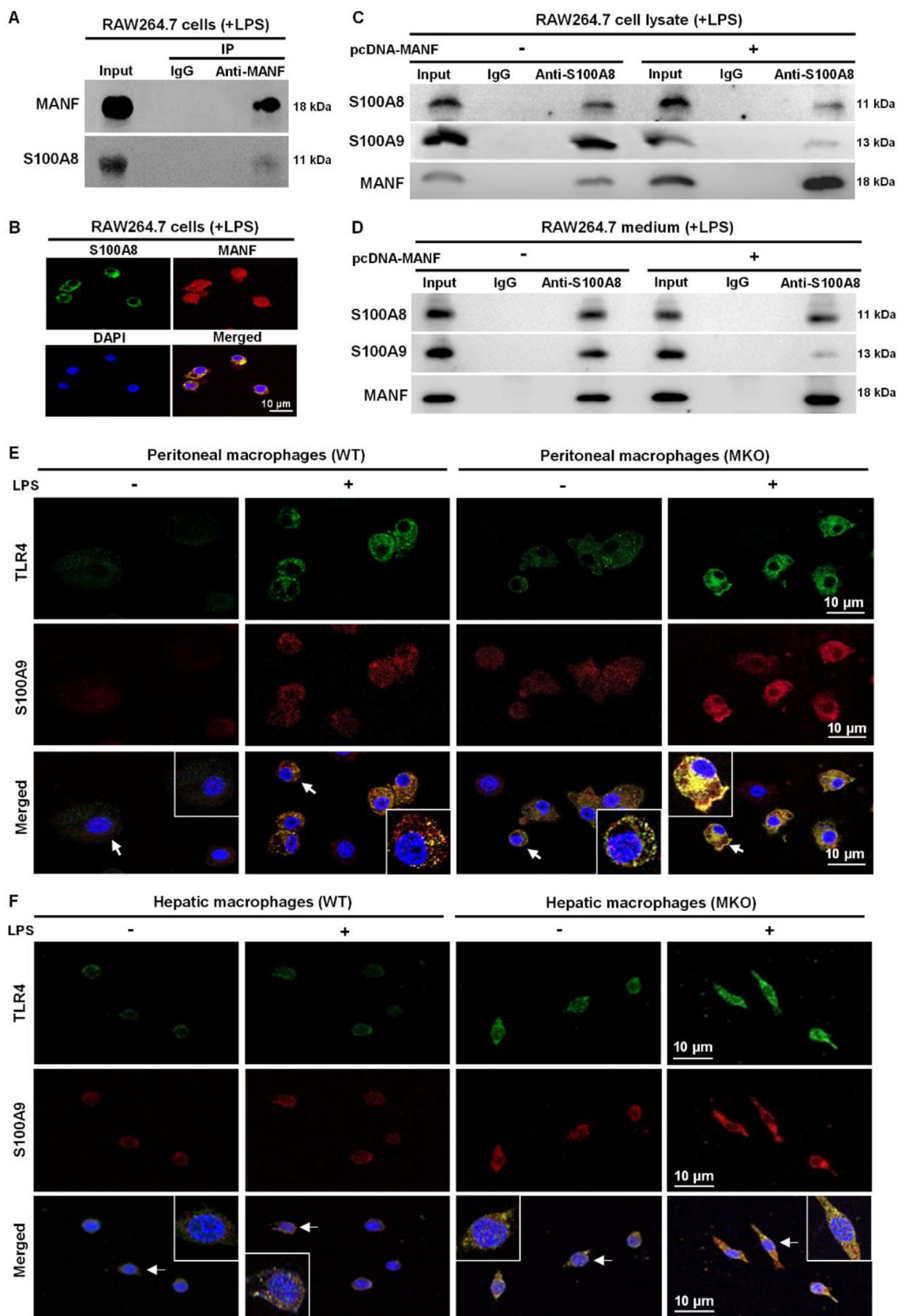


Figure 6 MANF interacts with S100A8 to impede S100A8/A9-TLR4 signaling. (A) Interaction of MANF and S100A8 was detected by Co-IP. (B) Colocalization of MANF (red) and S100A8 (green) was detected by immunofluorescent staining. DAPI (blue) was used to stain nuclei. (C, D) MANF overexpression inhibited intracellular (C) and extracellular (D) interaction of S100A9 and S100A8 detected by Co-IP with anti-S100A8.

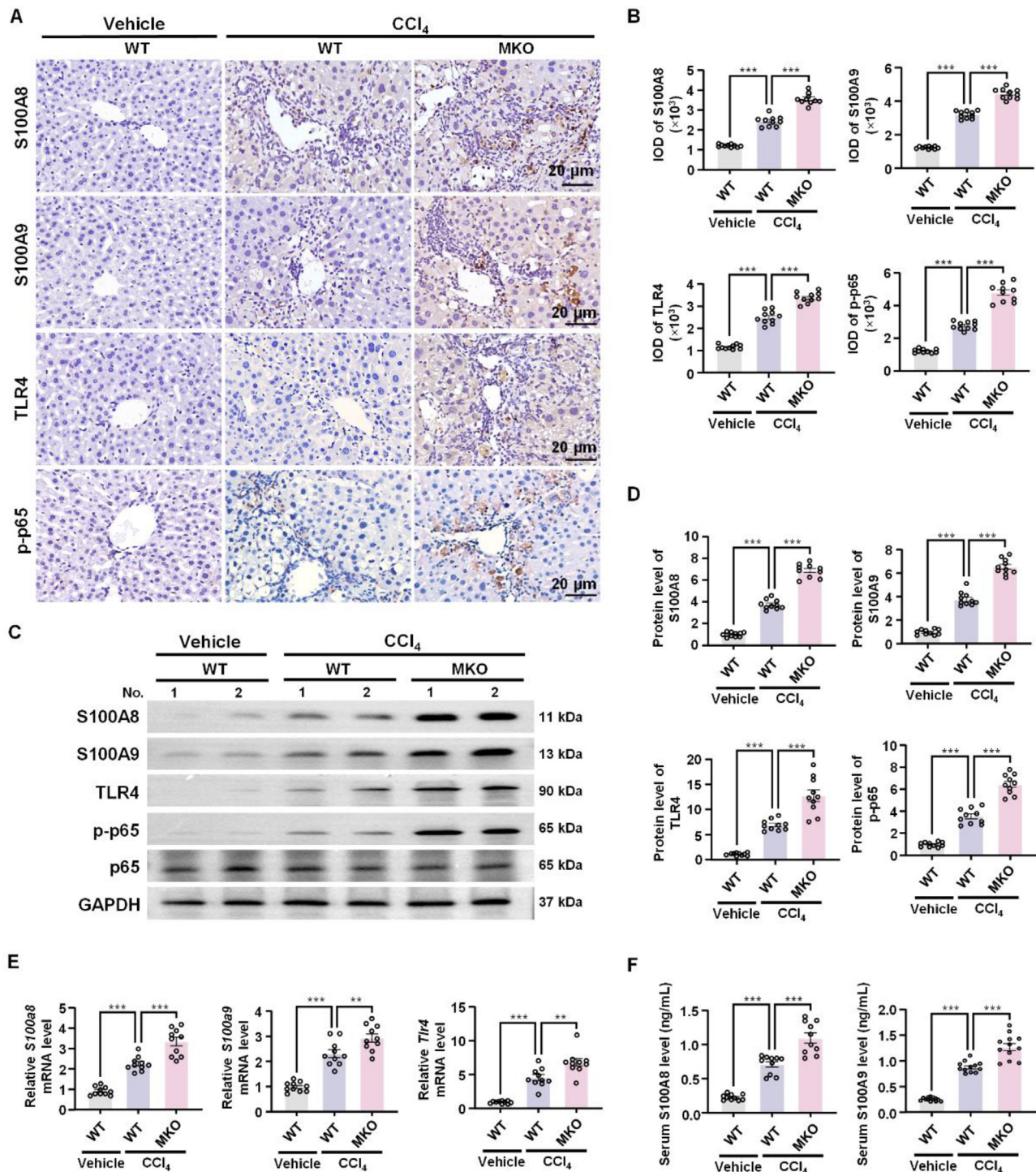


Figure 7 MANF deficiency in myeloid cells activates S100A8/A9-TLR4 signal pathway in mice with liver fibrosis. (A) MANF deficiency in myeloid cells upregulated hepatic S100A8, S100A9, TLR4 and p-p65 levels detected by using immunohistochemistry assay. (B) The quantitative data in panel A. (C) S100A8, S100A9, TLR4, p-p65 and p65 were detected by Western blot. (D) The quantitative data in panel C. (E) *S100a8*, *S100a9*, and *Tlr4* mRNA levels were detected by qPCR. (F) MANF deficiency in myeloid cells increased serum S100A8 and S100A9 levels. Serum S100A8 and S100A9 levels were detected by ELISA. Data are expressed as mean \pm SEM, $n = 10$; ** $P < 0.01$, *** $P < 0.001$. WT, wild type; HKO, MANF knockout in hepatocytes; MKO, MANF knockout in myeloid cells; CCl₄, carbon tetrachloride.

(E, F) MANF deficiency in macrophages increased colocalization of S100A9 and TLR4 in peritoneal macrophages (E) and hepatic macrophages (F) by detecting TLR4 (green) and S100A9 (red), $n = 5$. DAPI (blue) was used to stain nuclei. WT, wild type; MKO, MANF knockout in myeloid cells; LPS, lipopolysaccharide.

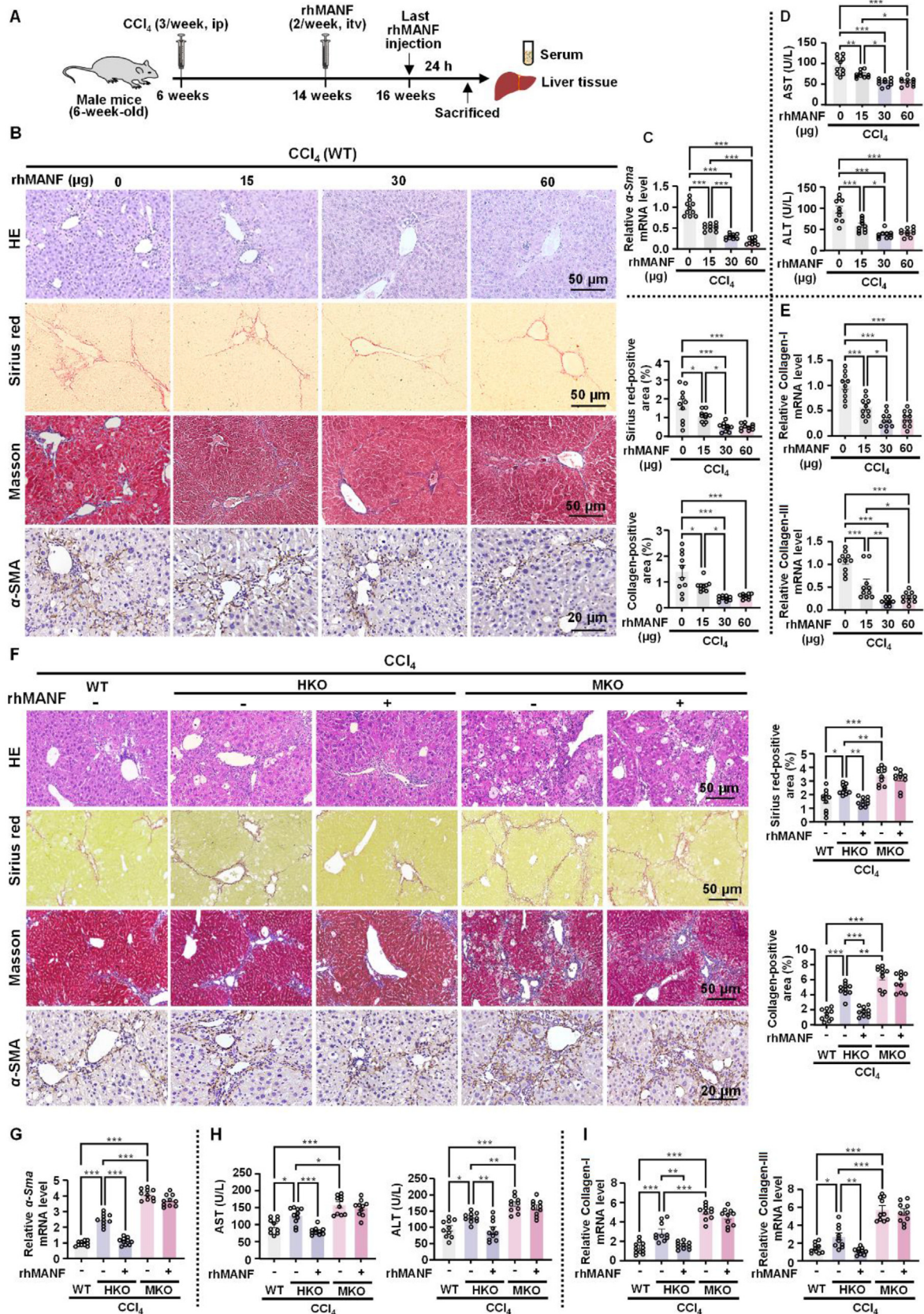


Figure 8 Recombinant human MANF attenuates CCl₄-induced hepatic fibrosis. (A) Strategy for rhMANF administration. (B) MANF inhibited liver fibrosis. HE, Sirius red, and Masson staining were performed, and the positive area were calculated. α -SMA was detected by immunohistochemistry assay. (C) MANF decreased hepatic α -Sma mRNA level detected by qPCR. (D) MANF decreased serum AST and ALT levels. (E)

3.6. MANF interacts with S100A8 to inhibit S100A8/A9 heterodimer formation

Next, interacting proteins of MANF were identified by liquid chromatography-tandem mass spectrometry (LC-MS) following immunoprecipitation (IP) in HepG2 hepatoma cells. Interestingly, S100A8, as a heterodimer with S100A9 (S100A8/A9) involving in inflammation *via* binding to TLR4^{31,32}, was among the candidate proteins (Supporting Information Fig. S7). The interaction between MANF and S100A8 was confirmed by Co-IP and immunofluorescent staining in RAW264.7 cells (Fig. 6A and B). More interestingly, MANF overexpression enhanced the interaction of MANF and S100A8, while the level of S100A9 interacting with S100A8 was decreased either in cells or in the medium (Fig. 6C and D), indicating both intracellular and secreted MANF can competitively bind S100A8 with S100A9 to inhibit the formation of S100A8/A9 heterodimer. Furthermore, the colocalization of S100A9 and TLR4 in the peritoneal and hepatic macrophages isolated from MKO mice was increased after LPS stimulation, compared with that from WT mice (Fig. 6E and F). Additionally, the colocalization of S100A8 and S100A9, as well as S100A9 and TLR4 were increased in the hepatic macrophages isolated from MKO mice with hepatic fibrosis than that from WT mice (Supporting Information Fig. S8A and S8B), suggesting MANF deficiency enhances the interaction of S100A9 and TLR4 in macrophages. These results indicate that MANF competitively binds S100A8 with S100A9 to disturb S100A8/A9 heterodimer formation in hepatic macrophages, which could further impede S100A8/A9-TLR4-NF- κ B signaling.

Consistently, S100A8, S100A9, and TLR4 levels in fibrotic liver tissue were upregulated by CCl₄ induction, and MANF deficiency in myeloid cells further increased the levels of S100A8, S100A9, and TLR4 (Fig. 7A–E). The serum S100A8 and S100A9 levels were also elevated in MKO mice compared to WT mice with CCl₄ treatment (Fig. 7F). Meanwhile, NF- κ B p65 phosphorylation was increased in MKO mice compared to WT mice with or without hepatic fibrosis (Fig. 7A–D and Supporting Information Fig. S9). There was no difference in hepatic levels of S100A8, S100A9 and TLR4 between WT and MKO without CCl₄ treatment (Fig. S9).

3.7. Recombinant human MANF inhibits CCl₄-induced hepatic fibrosis

To further confirm the protective effect of MANF against hepatic fibrosis, we firstly administrated rhMANF to the WT mice by tail vein injection twice a week for 2 weeks after CCl₄ challenge (Fig. 8A). We found that rhMANF at the doses of 15, 30, and 60 μ g per mouse remarkably attenuated CCl₄-induced liver injury and fibrosis in WT mice. The recovery from liver injury was assessed by histological repair using HE staining (Fig. 8B) and the decrease in serum AST and ALT levels (Fig. 8D). The effect of rhMANF on amelioration of liver fibrosis was reflected by the

reduced collagen area of Sirius red, Masson staining, and α -SMA protein level (Fig. 8B), as well as the decreased mRNA levels of α -Sma, collagen-I and -III (Fig. 8C and E). Recombinant human MANF at the doses of 30 and 60 μ g was more effective than that at the dose of 15 μ g. Similarly, rhMANF administration significantly relieved hepatic fibrosis in HKO mice (Fig. 8F–I). Unexpectedly, we found rhMANF had less effect on hepatic fibrosis in MKO mice with more severe liver fibrosis (Fig. 8F–I). Therefore, the ameliorating effect of rhMANF in CCl₄-induced liver fibrosis occurs mainly in WT and HKO mice.

3.8. Recombinant human MANF inhibits HSCs activation

To further confirm the effect of MANF on HSCs activation, rhMANF was used to treat primarily cultured HSCs isolated from WT mice. TNF- α (20 ng/mL) was used to activate the primary HSCs for 6 h following treatment with rhMANF (0, 5, 10, and 20 μ g/mL) for 2 h. We found that rhMANF was able to enter HSCs (Fig. 9C), and three concentrations of rhMANF inhibited TNF- α -induced upregulation of α -SMA, TIMP1 and 2 (Fig. 9A and B and Supporting Information Fig. S10A). In addition, immunofluorescent staining assay also demonstrated that rhMANF reduced the number and fluorescence intensity of α -SMA-positive HSCs (Fig. 9C and Fig. S10B). Recombinant human MANF at the doses of 10 and 20 μ g showed the greater effect to inhibit primary HSCs activation than that rhMANF at the dose of 5 μ g. So, the primary HSCs isolated from WT and MKO mice with hepatic fibrosis were treated with rhMANF (10 μ g/mL) *in vitro* to further verify the effect of MANF on HSCs activation. Results showed that the activation of HSCs was also inhibited after rhMANF treatment *in vitro* (Supporting Information Fig. S11A–S11E). These findings suggest that rhMANF restrains HSCs activation, which may attenuate hepatic fibrosis.

3.9. Hepatic macrophages-secreted MANF inhibits HSCs activation

Next, we further investigated whether MANF secreted from hepatic macrophages could induce HSCs activation *in vitro*. The hepatic macrophages isolated from WT and MKO mice were primarily cultured. After cell adhesion, LPS (0.5 μ g/mL) was added to the medium for 6 h, after which the medium was collected to treat the primary HSCs (Fig. 9D). Our data reveal that the medium collected from the cultured macrophages of MKO mice induced primary HSCs to produce higher levels of α -SMA, TIMP1 and 2 than that from the macrophages of WT mice (Fig. 9E–H and Fig. S10C). Consistently, LPS stimulation induced the macrophages of MKO mice to produce more TNF- α , IL-1 β , and CCL2 into the medium than WT mice (Fig. 9I–L). The major difference between the mediums from the primarily cultured macrophages of WT and MKO mice was the levels of MANF in the mediums, due to the lack of MANF in hepatic macrophages of MKO mice (Fig. 9M). These results suggest that

MANF inhibited hepatic Collagen-I and -III mRNA levels detected by qPCR. (F) MANF inhibited CCl₄-induced hepatic fibrosis in HKO mice. WT and MKO mice were used as the controls. HE, Sirius red, and Masson staining were performed and positive area were calculated. α -SMA was detected by immunohistochemistry. (G) MANF inhibited CCl₄-induced α -Sma mRNA expression detected by qPCR in HKO mice. (H) MANF inhibited CCl₄-induced serum AST and ALT increase in HKO mice. (I) MANF inhibited CCl₄-induced hepatic Collagen-I and -III mRNA expression in HKO mice. Data are expressed as mean \pm SEM, $n = 10$; * $P < 0.05$, ** $P < 0.01$, *** $P < 0.001$. WT, wild type; HKO, MANF knockout in hepatocytes; MKO, MANF knockout in myeloid cells; CCl₄, carbon tetrachloride.

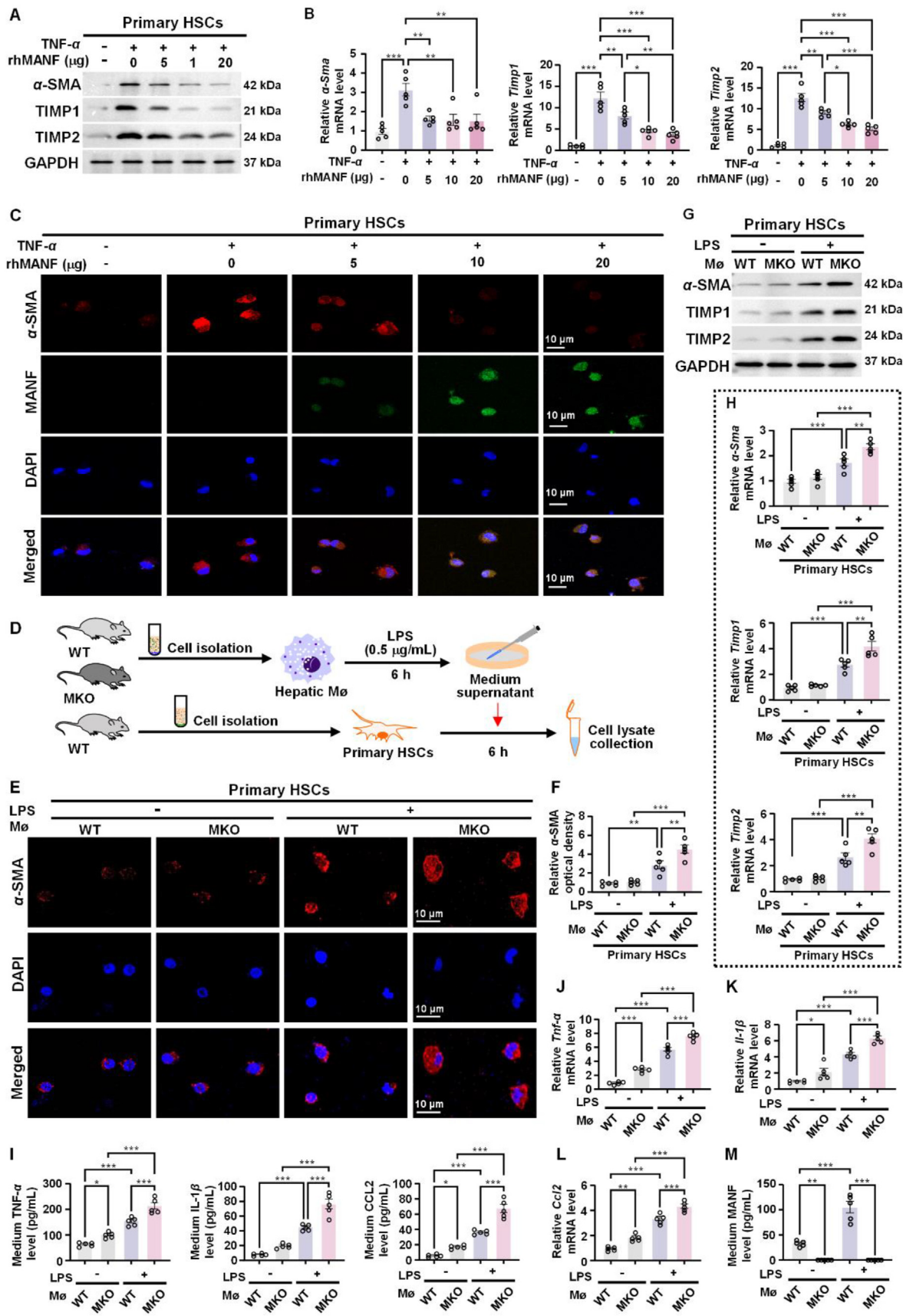


Figure 9 MANF inhibits primary HSCs activation *in vitro*. (A, B) Recombinant human MANF inhibited TNF- α -induced protein (A) and mRNA (B) levels of α -SMA, TIMP1, and TIMP2 in primary HSCs detected by Western blot and qPCR, respectively. (C) Recombinant human

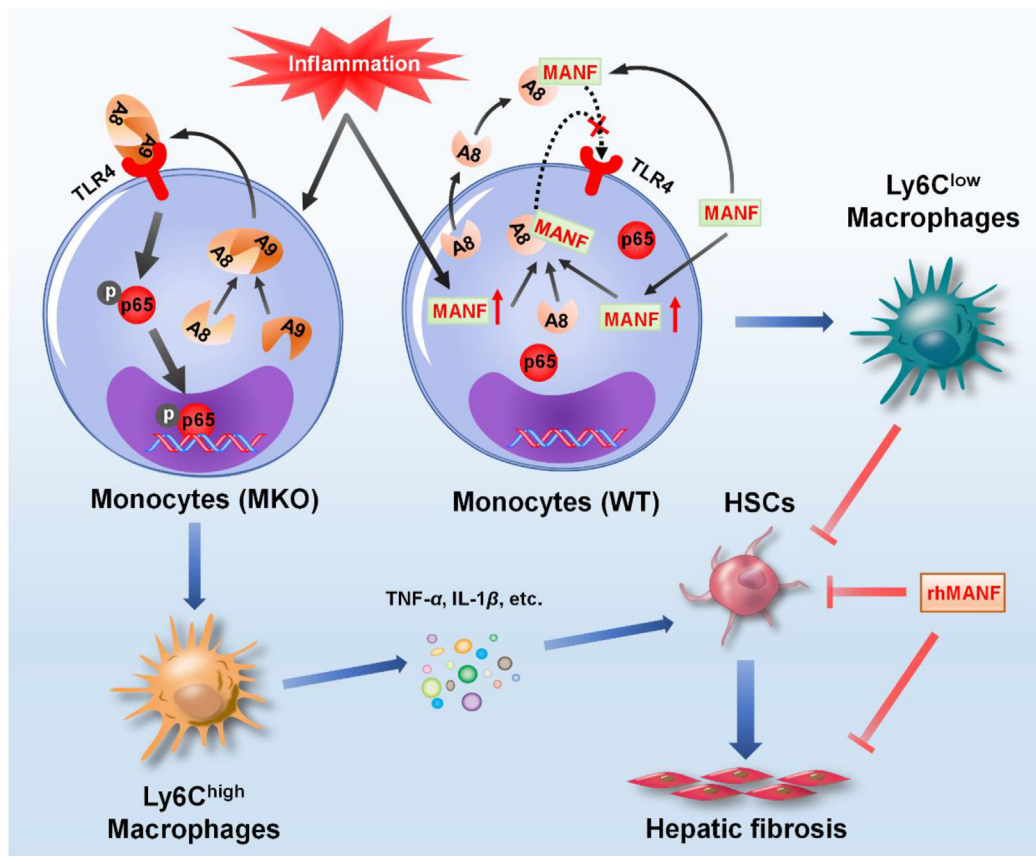


Figure 10 Schematic model for the regulation of MANF in hepatic fibrosis. In WT mice, hepatic inflammation upregulates MANF expression and secretion, and S100A8 preferentially interacts with intracellular and extracellular MANF to form S100A8/MANF complex, which disturbs the formation of S100A8/A9 heterodimer, subsequently blocks S100A8/A9–TLR4–NF- κ B signal pathway. As a result, the monocytes are induced to differentiate Ly6C^{low} macrophages that can inhibit HSCs activation and hepatic fibrosis. Additionally, rhMANF can directly restrain HSCs activation and hepatic fibrosis. However, in MKO mice, hepatic inflammation activates S100A8/A9–TLR4–NF- κ B signal, which drives monocytes to differentiate towards Ly6C^{high} macrophages. In this way, HSCs are activated by the inflammatory cytokines produced by Ly6C^{high} macrophages, which leads to hepatic fibrosis.

hepatic macrophages-secreted MANF exerts a suppressive role in HSCs activation.

4. Discussion

4.1. Protective effects of MANF on hepatic fibrosis

A previous study reported that hepatic MANF level decreases with aging, and MANF supplementation can alleviate liver aging, including prevention of hepatic steatosis¹⁷. Based on this observation, MANF was speculated to ameliorate hepatic inflammation and fibrosis¹⁷. Here, we reveal for the first time that MANF

facilitates to restrain hepatic inflammation and fibrosis. In our study, we found an interesting result showing that MANF deficiency in myeloid cells exerts a greater effect on hepatic inflammation and fibrosis than that in hepatocytes. It is well known, hepatocytes are the predominant cell type in liver, accounting for about 80% of hepatic cells³³. Our data also exhibited that MANF was mainly expressed in hepatocytes and hepatic macrophages, but not in HSCs and hepatic granulocytes under hepatic fibrosis. Therefore, the majority of hepatic MANF is supposed to come from hepatocytes based on its size and population. An important question then arises as to why a small amount of MANF derived from hepatic macrophages plays a more important role in liver

MANF reduced TNF- α -induced α -SMA expression in HSCs. His-MANF (green) and α -SMA (red) were detected by immunofluorescent assay. DAPI (blue) was used to stain nuclei. (D) Strategy for primary HSCs treatment. The medium collected from hepatic macrophages was used to treat primary HSCs isolated from WT mice. (E) The medium collected from hepatic macrophages of MKO mice increased α -SMA level (red) in HSCs. DAPI (blue) was used to stain nuclei. (F) The quantitative data in panel E. (G, H) The medium collected from MANF-deficient macrophages increased α -SMA, TIMP1, and TIMP2 protein (G) and mRNA (H) levels of the primary HSCs detected by Western blot and qPCR, respectively. (I) MANF deficiency in hepatic macrophages increased TNF- α , IL-1 β , and CCL2 secretion in the medium detected by ELISA. (J–L) MANF deficiency in hepatic macrophages increased mRNA levels of *Tnf- α* (J), *Il-1 β* (K) and *Ccl2* (L) detected by qPCR. (M) Medium MANF was detected by ELISA. Data are expressed as mean \pm SEM, $n = 5$; * $P < 0.05$, ** $P < 0.01$, *** $P < 0.001$. rhMANF, recombinant human MANF; WT, wild type; MKO, MANF knockout in myeloid cells; LPS, lipopolysaccharide; M ϕ , macrophage.

fibrosis. This may be due to the role of macrophages in the regulation of liver inflammation and the effect of MANF on it, in other words, MANF may play an important role in controlling macrophages' function that is not dependent on the amount of intracellular MANF. It is also possible that MANF derived from hepatocytes and hepatic macrophages may exert their liver protection effects in different manners. The detailed mechanism needs further research in the future.

Administration of rhMANF alleviated CCl₄-induced hepatic fibrosis in WT and HKO mice, but less effect in MKO mice, possibly due to the different degrees of hepatic fibrosis among WT, HKO, and MKO mice. The most severe hepatic fibrosis was found in MKO mice that could not be recovered by rhMANF. Therefore, we suggest that rhMANF has a remarkable therapeutic effect on early hepatic fibrosis, but has limited effect on severe hepatic fibrosis in the later phase.

4.2. Paracrine regulation of MANF in HSCs

In this study, we found that MANF was not expressed in HSCs, suggesting that MANF might exert its effect on HSCs *via* paracrine secretion. To clarify this hypothesis, we collected the medium from the primarily cultured hepatic macrophages of MKO mice to treat the primarily cultured HSCs. The results showed that MANF-lacking medium promoted HSCs activation, suggesting MANF secreted from macrophages can regulate HSCs *via* paracrine mechanism. The medium from the primary macrophages contains other cytokines except for MANF. We also found MANF can inhibit proinflammatory macrophages activation and reduce cytokines production. Therefore, HSCs activation by the medium of the primary macrophages of MKO mice may be attribute to MANF deficiency as well as increased cytokine levels. Exogenous rhMANF can inhibit the activation of primarily cultured HSCs activation *in vitro*, supporting the notion that MANF regulates HSCs activation *via* paracrine mechanism.

4.3. Suppressive effect of MANF in hepatic macrophage differentiation

The liver is an important immune organ containing Kupffer cells, dendritic cells (DCs), and other types of immune cells³⁴. Among the factors affecting HSCs activation and ECM metabolism, hepatic immune microenvironment and innate immunity have been implicated as key regulators³⁵. Hepatic macrophage differentiation and heterogeneity have been demonstrated to contribute greatly to liver inflammation, damage repair, and hepatic fibrosis^{36–38}. The plasma membrane glycoprotein Ly6C has been widely used to distinguish macrophage subtypes in mice. Ly6C^{high} monocytes belong to pro-inflammatory monocytes that can be recruited to inflamed tissues^{30,39}, and the circulatory Ly6C^{low} monocytes can be infiltrated into tissues for macrophage supplementation⁴⁰. CD11b^{high}Ly6C^{high} mono-macrophages activate HSCs for pro-fibrogenesis; conversely, CD11b^{high}Ly6C^{low} mono-macrophages accelerate fiber degradation and tissue recovery in liver. Early Ly6C^{high} pro-inflammatory and fibrogenic macrophages differentiate into later Ly6C^{low} anti-fibrosis macrophages³⁰. However, what factors dominate the phenotypes of hepatic macrophages differentiation are still unclear. MANF has been found to be upregulated in inflammatory diseases and suggested to act as a negative regulator of inflammation *via* interacting with NF- κ B p65 and subsequently inhibiting NF- κ B target genes transcription^{18,19}. MANF has also been reported to be a

regulator of macrophage pro-inflammatory/anti-inflammatory differentiation in retinal tissue repair⁴¹. Our data revealed that MANF deficiency in hepatocytes and hepatic macrophages promoted the inflammatory phenotype transformation of macrophages and HSCs activation, and macrophage-derived MANF is clearly more potent than hepatocyte-derived MANF in inhibiting HSCs activation, suggesting that MANF may play an important role in hepatic macrophages-mediated HSCs activation.

4.4. Negative regulation of MANF in S100A8/A9-TLR4 signaling

S100A8 and S100A9, the calcium-binding proteins belonging to S100 protein family, have been implicated in modulating the immune response mainly in the form of heterodimers^{42,43}. S100A8 and S100A9 have been proven to be constitutively expressed in neutrophils, myeloid-derived dendritic cells, and monocytes. Furthermore, S100A8/A9 participates in innate immunity *via* binding to TLR4^{31,32}. Therefore, S100A8 and S100A9 are potential regulators for mono-macrophage differentiation in the liver. Here, we found that S100A8/A9 expression is greatly increased in response to hepatic inflammation, and S100A8/A9 was involved in macrophage differentiation by interacting with mono-macrophage-derived MANF. S100A8/A9 functions as a ligand of TLR4 and activates multiple TLR4-related inflammatory signaling pathways^{31,44}. It has also been reported that S100A9 is an effective factor in suppressing pro-inflammatory macrophage polarization⁴⁵. As a novel S100A8 interacting protein, MANF could compete with S100A9 for S100A8 binding to restrain S100A8/A9 heterodimer formation. MANF deficiency in mono-macrophages increased S100A9 membrane localization along with TLR4, indicating that the interaction of MANF and S100A8 might negatively affect S100A8/A9–TLR4–NF- κ B intracellular signaling to restrict Ly6C^{high} pro-inflammatory macrophage differentiation and activation.

Taken together, this study explores the influence of MANF, especially myeloid-derived MANF, on inflammation and fibrogenesis in the liver. With the predefined role of MANF in NF- κ B inhibition, here, we propose a “dual channel” model of MANF activity on NF- κ B signaling suppression to regulate hepatic macrophage differentiation. In upstream signaling, MANF restrains TLR4 activation by binding to S100A8 and inhibiting S100A8/A9 heterodimer formation (Fig. 10); while in downstream, MANF blocks NF- κ B target gene transcription *via* interacting with NF- κ B p65 DNA binding domain. Our findings are beneficial for seeking a potent anti-inflammatory and anti-fibrosis factor for the treatment of hepatic fibrosis, as well as for further understanding the precise mechanism of how MANF regulates macrophage differentiation.

5. Conclusions

We demonstrated that mesencephalic astrocyte-derived neurotrophic factor (MANF), including hepatic cells-derived MANF and recombinant human MANF (rhMANF) protects against mouse liver fibrosis by inhibiting pro-inflammatory Ly6C^{high} macrophages infiltration and differentiation, which exerts a direct effect on HSCs. Mechanistically, MANF competitively interacts with S100A8 to inhibit S100A8/A9 heterodimer formation, subsequently attenuating S100A8/A9–TLR4–NF- κ B signaling activation in hepatic pro-inflammatory macrophages.

Acknowledgments

We would like to thank Prof. Jia Luo from the University of Kentucky for supplying MANF conditional knockout mice. This work was supported by the National Natural Science Foundation of China (81973336) and the Joint Fund of the National Natural Science Foundation of China (U21A20345).

Authors contributions

Yuxian Shen and Yang Sun designed the study, supervised the experiments, and revised the manuscript draft. Chao Hou and Dong Wang performed the experiments, analyzed the data and wrote the manuscript. Petek Ballar revised the manuscript draft and edited the language. Mingxia Zhao, Xinru Zhang, Qiong Mei, Wei Wang, Xiang Li, Qiang Sheng, Sa Xu and Fuyan Wang performed the experiments. Jun Liu established MANF conditional knockout mice. Chuansheng Wei, Xinru Zhang and Wei Wang fed mice. Yujun Shen and Juntang Shao participated in the animal studies. Yi Yang and Peng Wang conducted the LC/MS experiment and analyzed the data.

Conflicts of interest

The authors declare no conflicts of interest.

Appendix A. Supporting information

Supporting data to this article can be found online at <https://doi.org/10.1016/j.apsb.2023.07.027>.

References

- Xia SW, Wang ZM, Sun SM, Su Y, Li ZH, Shao JJ, et al. Endoplasmic reticulum stress and protein degradation in chronic liver disease. *Pharmacol Res* 2020;**161**:105218.
- Kisseleva T, Brenner D. Molecular and cellular mechanisms of liver fibrosis and its regression. *Nat Rev Gastroenterol Hepatol* 2021;**18**:151–66.
- Mahdinloo S, Kiaie SH, Amiri A, Hemmati S, Valizadeh H, Zakeri-Milani P. Efficient drug and gene delivery to liver fibrosis: rationale, recent advances, and perspectives. *Acta Pharm Sin B* 2020;**10**:1279–93.
- Atzori L, Poli G, Perra A. Hepatic stellate cell: a star cell in the liver. *Int J Biochem Cell Biol* 2009;**41**:1639–42.
- Zheng WD, Zhang LJ, Shi MN, Chen ZX, Chen YX, Huang YH, et al. Expression of matrix metalloproteinase-2 and tissue inhibitor of metalloproteinase-1 in hepatic stellate cells during rat hepatic fibrosis and its intervention by IL-10. *World J Gastroenterol* 2005;**11**:1753–8.
- Nieto N, Dominguez-Rosales JA, Fontana L, Salazar A, Armendariz-Borunda J, Greenwel P, et al. Rat hepatic stellate cells contribute to the acute-phase response with increased expression of alpha1(I) and alpha1(IV) collagens, tissue inhibitor of metalloproteinase-1, and matrix-metalloproteinase-2 messenger RNAs. *Hepatology* 2001;**33**:597–607.
- Tanwar S, Rhodes F, Srivastava A, Trembling PM, Rosenberg WM. Inflammation and fibrosis in chronic liver diseases including non-alcoholic fatty liver disease and hepatitis C. *World J Gastroenterol* 2020;**26**:109–33.
- Koyama Y, Brenner DA. Liver inflammation and fibrosis. *J Clin Invest* 2017;**127**:55–64.
- Zhu Y, Liu H, Zhang M, Guo GL. Fatty liver diseases, bile acids, and FXR. *Acta Pharm Sin B* 2016;**6**:409–12.
- Yang W, Shen Y, Chen Y, Chen L, Wang L, Wang H, et al. Mesencephalic astrocyte-derived neurotrophic factor prevents neuron loss via inhibiting ischemia-induced apoptosis. *J Neurol Sci* 2014;**344**:129–38.
- Tseng KY, Anttila JE, Khodosevich K, Tuominen RK, Lindahl M, Domanskyi A, et al. MANF promotes differentiation and migration of neural progenitor cells with potential neural regenerative effects in stroke. *Mol Ther* 2018;**26**:238–55.
- Petrova P, Raibekas A, Pevsner J, Vigo N, Anafi M, Moore MK, et al. MANF: a new mesencephalic, astrocyte-derived neurotrophic factor with selectivity for dopaminergic neurons. *J Mol Neurosci* 2003;**20**:173–88.
- Apostolou A, Shen Y, Liang Y, Luo J, Fang S. Armet, a UPR-upregulated protein, inhibits cell proliferation and ER stress-induced cell death. *Exp Cell Res* 2008;**314**:2454–67.
- Yang Y, Wang P, Zhang C, Huang F, Pang G, Wei C, et al. Hepatocyte-derived MANF alleviates hepatic ischaemia–reperfusion injury via regulating endoplasmic reticulum stress-induced apoptosis in mice. *Liver Int* 2021;**41**:623–39.
- Chhetri G, Liang Y, Shao J, Han D, Yang Y, Hou C, et al. Role of mesencephalic astrocyte-derived neurotrophic factor in alcohol-induced liver injury. *Oxid Med Cell Longev* 2020;**2020**:9034864.
- Wang P, Yang Y, Pang G, Zhang C, Wei C, Tao X, et al. Hepatocyte-derived MANF is protective for rifampicin-induced cholestatic hepatic injury via inhibiting ATF4-CHOP signal activation. *Free Radic Biol Med* 2021;**162**:283–97.
- Sousa-Victor P, Neves J, Cedron-Craft W, Ventura PB, Liao CY, Riley RR, et al. MANF regulates metabolic and immune homeostasis in ageing and protects against liver damage. *Nat Metab* 2019;**1**:276–90.
- Chen L, Feng L, Wang X, Du J, Chen Y, Yang W, et al. Mesencephalic astrocyte-derived neurotrophic factor is involved in inflammation by negatively regulating the NF- κ B pathway. *Sci Rep* 2015;**5**:8133.
- Shen QY, Wang D, Xu HY, Wei CS, Xiao XY, Liu J, et al. Mesencephalic astrocyte-derived neurotrophic factor attenuates acute lung injury via inhibiting macrophages' activation. *Biomed Pharmacother* 2022;**150**:112943.
- Liu J, Wu Z, Han D, Wei C, Liang Y, Jiang T, et al. Mesencephalic astrocyte-derived neurotrophic factor inhibits liver cancer through small ubiquitin-related modifier (SUMO)ylation-related suppression of NF- κ B/Snail signaling pathway and epithelial–mesenchymal transition. *Hepatology* 2020;**71**:1262–78.
- Chen X, Li HD, Bu FT, Li XF, Chen Y, Zhu S, et al. Circular RNA circFBXW4 suppresses hepatic fibrosis via targeting the miR-18b-3p/FBXW7 axis. *Theranostics* 2020;**10**:4851–70.
- Ma PF, Gao CC, Yi J, Zhao JL, Liang SQ, Zhao Y, et al. Cytotherapy with M1-polarized macrophages ameliorates liver fibrosis by modulating immune microenvironment in mice. *J Hepatol* 2017;**67**:770–9.
- Xu HY, Jiao YH, Li SY, Zhu X, Wang S, Zhang YY, et al. Hepatocyte-derived MANF mitigates ethanol-induced liver steatosis in mice via enhancing ASS1 activity and activating AMPK pathway. *Acta Pharmacol Sin* 2023;**44**:157–68.
- Pan G, Gao Y, Ye J, Jiang T, Shen Y, Shen Y. Study on correlation between MANF expression levels and the grade of liver fibrosis. *Acta Univ Med Anhui* 2015;**50**:78–82.
- Ge X, Arriaza E, Magdaleno F, Antoine DJ, Dela Cruz R, Theise N, et al. High mobility group box-1 drives fibrosis progression signaling via the receptor for advanced glycation end products in mice. *Hepatology* 2018;**68**:2380–404.
- Lee UE, Friedman SL. Mechanisms of hepatic fibrogenesis. *Best Pract Res Clin Gastroenterol* 2011;**25**:195–206.
- Yoshida K, Matsuzaki K. Differential regulation of TGF- β /Smad signaling in hepatic stellate cells between acute and chronic liver injuries. *Front Physiol* 2012;**3**:53.
- Seki E, De Minicis S, Osterreicher CH, Kluwe J, Osawa Y, Brenner DA, et al. TLR4 enhances TGF- β signaling and hepatic fibrosis. *Nat Med* 2007;**13**:1324–32.
- Garantziotis S, Savani RC. Hyaluronan biology: a complex balancing act of structure, function, location and context. *Matrix Biol* 2019;**78**:1–10.

30. Ramachandran P, Pellicoro A, Vernon MA, Boulter L, Aucott RL, Ali A, et al. Differential Ly-6C expression identifies the recruited macrophage phenotype, which orchestrates the regression of murine liver fibrosis. *Proc Natl Acad Sci U S A* 2012;**109**:E3186–95.
31. Vogl T, Tenbrock K, Ludwig S, Leukert N, Ehrhardt C, van Zoelen MA, et al. Mrp8 and Mrp14 are endogenous activators of Toll-like receptor 4, promoting lethal, endotoxin-induced shock. *Nat Med* 2007;**13**:1042–9.
32. Guo Q, Zhao Y, Li J, Liu J, Yang X, Guo X, et al. Induction of alarmin S100A8/A9 mediates activation of aberrant neutrophils in the pathogenesis of COVID-19. *Cell Host Microbe* 2021;**29**:222–235.e4.
33. Ben-Moshe S, Itzkovitz S. Spatial heterogeneity in the mammalian liver. *Nat Rev Gastroenterol Hepatol* 2019;**16**:395–410.
34. Guillems M, Bonnardel J, Haest B, Vanderborght B, Wagner C, Remmerie A, et al. Spatial proteogenomics reveals distinct and evolutionarily conserved hepatic macrophage niches. *Cell* 2022;**185**:379–396.e38.
35. Holt AP, Salmon M, Buckley CD, Adams DH. Immune interactions in hepatic fibrosis. *Clin Liver Dis* 2008;**12**:861–82.
36. Ehling J, Bartneck M, Wei X, Gremse F, Fecht V, Mockel D, et al. CCL2-dependent infiltrating macrophages promote angiogenesis in progressive liver fibrosis. *Gut* 2014;**63**:1960–71.
37. Ju C, Tacke F. Hepatic macrophages in homeostasis and liver diseases: from pathogenesis to novel therapeutic strategies. *Cell Mol Immunol* 2016;**13**:316–27.
38. Dong X, Feng Y, Xu D, Zhang M, Wen X, Zhao W, et al. Targeting macrophagic 17 β -HSD7 by fenretinide for the treatment of nonalcoholic fatty liver disease. *Acta Pharm Sin B* 2023;**13**:142–56.
39. Graubardt N, Vugman M, Mouhadeb O, Caliani G, Pasmanik-Chor M, Reuveni D, et al. Ly6C^{hi} monocytes and their macrophage descendants regulate neutrophil function and clearance in acetaminophen-induced liver injury. *Front Immunol* 2017;**8**:626.
40. Tacke F, Zimmermann HW. Macrophage heterogeneity in liver injury and fibrosis. *J Hepatol* 2014;**60**:1090–6.
41. Neves J, Zhu J, Sousa-Victor P, Konjikusic M, Riley R, Chew S, et al. Immune modulation by MANF promotes tissue repair and regenerative success in the retina. *Science* 2016;**353**:aaf3646.
42. Wang S, Song R, Wang Z, Jing Z, Wang S, Ma J. S100A8/A9 in inflammation. *Front Immunol* 2018;**9**:1298.
43. Lagasse E, Weissman IL. Mouse MRP8 and MRP14, two intracellular calcium-binding proteins associated with the development of the myeloid lineage. *Blood* 1992;**79**:1907–15.
44. Deguchi A, Tomita T, Ohto U, Takemura K, Kitao A, Akashi-Takamura S, et al. Eritoran inhibits S100A8-mediated TLR4/MD-2 activation and tumor growth by changing the immune microenvironment. *Oncogene* 2016;**35**:1445–56.
45. De Lorenzo BH, Godoy LC, Novaes e Brito RR, Pagano RL, Amorim-Dias MA, Grosso DM, et al. Macrophage suppression following phagocytosis of apoptotic neutrophils is mediated by the S100A9 calcium-binding protein. *Immunobiology* 2010;**215**:341–7.